



Synthesis, crystal structure and luminescence properties of lanthanide coordination polymers with a new semirigid bridging thenylsalicylamide ligand



Xue-Qin Song*, Li Wang, Meng-Meng Zhao, Xiao-Run Wang, Yun-Qiao Peng, Guo-Quan Cheng

School of Chemical and Biological Engineering, Lanzhou Jiaotong University, Lanzhou 730070, China

ARTICLE INFO

Article history:

Received 25 May 2013

Received in revised form

12 July 2013

Accepted 14 July 2013

Available online 26 July 2013

Keywords:

Salicylamide ligand

Lanthanide coordination polymer

Crystal structure

Luminescence properties

ABSTRACT

Two new lanthanide coordination polymers based on a semirigid bridging thenylsalicylamide ligand $\{[\text{Ln}_2\text{L}_3(\text{NO}_3)_6] \cdot (\text{C}_4\text{H}_8\text{O}_2)_2\}_\infty$ were obtained and characterized by elemental analysis, X-ray diffraction, IR and TGA measurements. The two compounds are isostructure and possess one dimensional trapezoid ladder-like chain built up from the connection of isolated $\text{LnO}_3(\text{NO}_3)_3$ polyhedra (distorted monocapped antisquare prism) through the ligand. The photoluminescence analysis suggest that there is an efficient ligand-to-Ln(III) energy transfer in Tb(III) complex and the ligand is an efficient “antenna” for Tb(III). From a more general perspective, the results demonstrated herein provide the possibility of controlling the formation of the desired lanthanide coordination structure to enrich the crystal engineering strategy and enlarge the arsenal for developing excellent luminescent lanthanide coordination polymers.

© 2013 Elsevier Inc. All rights reserved.

1. Introduction

Research into utilizing rare earth compounds in industrial, technological, and medical applications has been continuously growing over the last few decades. The interest is stimulated not only by their unique spectroscopic and magnetic properties, but also by their numerous applications in catalysts, magnets and luminescent materials [1–4]. Lanthanide coordination polymers in particular are promising materials because of the intrinsic physical properties of the trivalent lanthanide ions, such as color-pure luminescence, large paramagnetism, and the fact that the electrostatic nature of their coordination chemistry allows a large variety of symmetries and structural patterns to be obtained. One of the focal points for the design and exploitation of CPs is the rational choice and assembly of metal ions and versatile bridging organic ligands. In recent years, various organic ligands used for constructing lanthanide coordination polymers have been synthesized [5–10]. Among these numerous ligands, salicylamide ligands provide a fascinating prospect in preparing lanthanide-based CPs as a result of interesting chemical ability to form a wide variety of frameworks with different dimensionalities and sensitize lanthanide luminescence successfully [11].

We are interested in the synthesis and characterization of lanthanide complexes with flexible ligands incorporating salicylamide derivatives, and especially in how different types of flexible backbone as well as different terminal coordination sites can impact the structures and the luminescence properties [12]. As a continuation of our work with the lanthanide complex with salicylamide derivatives, we have successfully obtained a series of lanthanide coordination polymers of a semirigid bridging ligand with 1,4-dimethoxybenzene backbone and terminated with picolysalicylamide recently [11k]. With continued exploration, we reported herein two novel lanthanide coordination polymers of similar ligand with thenylsalicylamide terminal group, namely, 1,4-bis $\{[(2'-\text{thenylaminoformyl})\text{phenoxy}]methyl\}$ -2,5-bismethoxybenzene(L) (Scheme 1). As a result, two novel lanthanide coordination polymers, namely, $\{[\text{Gd}_2\text{L}_3(\text{NO}_3)_6] \cdot 2\text{C}_4\text{H}_8\text{O}_2\}_\infty$ (1), $\{[\text{Tb}_2\text{L}_3(\text{NO}_3)_6] \cdot 2\text{C}_4\text{H}_8\text{O}_2\}_\infty$ (2) were obtained and characterized by elemental analysis, X-ray diffraction analysis, IR spectroscopy and thermogravimetric (TGA) analysis. The two compounds are isostructural and crystallize in triclinic space group *P*-1. They possess one dimensional trapezoid ladder-like chain built up from the connection of isolated $\text{LnO}_3(\text{NO}_3)_3$ polyhedra (distorted monocapped antisquare prism) through the ligand, which further connected by C–H...O hydrogen bond to 3D supramolecular architectures. The lowest triplet state energy levels of the ligand was calculated from the phosphorescence spectra of the Gd(III) complex at 77 K. The results presented herein indicated that the new semirigid bridging ligand exhibited a good antennae effect to the Tb(III) ion due to efficient ligand to metal energy transfer.

* Corresponding author. Fax: +86 931 4938755.

E-mail addresses: songxq@mail.lzjtu.cn, songxueqin001@163.com (X.-Q. Song).

2. Experimental

2.1. Materials and instrumentation

Thenylamine and 1,4-bis(methoxy)-benzene was obtained from Alfa Aesar Co. Other commercially available chemicals were of analytical grade and were used without further purification. The lanthanide nitrates [13] were prepared according to the literature method.

Carbon, nitrogen, sulfur and hydrogen analyses were performed using an EL elemental analyzer. Melting points were determined on a Kofler apparatus. Infrared spectra ($4000\text{--}400\text{ cm}^{-1}$) were obtained with KBr discs on a Thermo Mattson FTIR spectrometer. Powder X-ray diffraction patterns (PXRD) were determined with Rigaku-D/Max-II X-ray diffractometer with graphite-monochromatized $\text{Cu-K}\alpha$ radiation. $^1\text{H NMR}$ spectra were recorded on a Bruker DRX 300 spectrometer in CDCl_3 solution with TMS as internal standard. Thermogravimetric analyses were carried out on a SDT Q600 thermogravimetric analyzer from room temperature to $600\text{ }^\circ\text{C}$. A platinum pan was used for heating the sample with a heating rate of $10\text{ }^\circ\text{C}/\text{min}$. Fluorescence measurements of the well grinded thick solid samples were made on FLS920 of Edinburgh Instrument. Samples were placed between two quartz cover slips and the excitation and emission slit of 0.2 nm were used. The 77 K solution-state phosphorescence spectra of the Gd(III) complex was recorded with solution samples (a 1: 1 Ethyl acetate–MeOH (v/v) mixture) loaded in a quartz tube inside a quartz-walled optical Dewar flask filled with liquid nitrogen in the phosphorescence mode on a Hitachi F-4500 spectrophotometer and equipped with a xenon lamp as the excitation source (front-face mode) [14]. Quantum yields were determined by an absolute method [15] using an integrating sphere on FLS920 of Edinburgh Instrument. The luminescence decays were recorded using a pumped dye laser (Lambda Physics model FL2002) as the excitation source. The nominal pulse width and the line width of the dye-laser output were 10 ns and 0.18 cm^{-1} , respectively. The emission of the sample was collected by two lenses in a monochromator (WDG30), detected by a photomultiplier and processed by a Boxcar Average (EGG model 162) in line with a microcomputer. Reported quantum yields and luminescence lifetimes are averages of at least three independent determinations. The estimated errors for quantum yields and luminescence lifetimes are 10%.

2.2. Synthesis of the ligand

The synthetic route for the ligand (L) is shown in Scheme 1. 2-thenylsalicylamide [16] and 1,4-bis(bromomethyl)-2,5-dimethoxy-benzene [17] was prepared according to the literature procedure.

To a solution of 2-thenylsalicylamide (2.45 g, 10.5 mmol) in dry acetone was added 1.52 g (11 mmol) dried K_2CO_3 , and the mixture was stirred for 30 min at room temperature, 1.61 g (5 mmol) 1,4-bis(bromomethyl)-2,5-dimethoxy-benzene in 20 ml of dry acetone was added dropwise in 30 min and the resulting solution stirred

and heated to reflux for 12 h. After cooling down, inorganic salts were separated by filtration and the solvent removed from the filtrate under reduced pressure. The crude product was recrystallized with ethyl acetate to give a white solid. 2.64 g, Yield 84%. m. p. $158\text{--}159\text{ }^\circ\text{C}$. Analytical data, Calc. for $\text{C}_{34}\text{H}_{32}\text{N}_2\text{O}_6\text{S}_2$: C, 64.95; H, 5.13; N, 4.46; S, 10.20; Found: C, 64.65; H, 5.14; N, 4.48; S, 10.23; IR (KBr, ν , cm^{-1}): 3375 (s), 2912(m), 2886(w), 1648 (s, C=O), 1597 (m), 1536 (s), 1480 (m), 1293 (s), 1226 (s, Ar–O), 752 (s). $^1\text{H NMR}$ (CDCl_3 , 300 MHz): δ : 4.75 (d, 4H, NHCH_2 , $J=5.2\text{ Hz}$), 5.26 (s, 4H, OCH_2), 6.93 (s, 2H, thiophene), 7.09 (m, 6H), 7.22 (m, 2H), 7.43 (dd, 2H), 7.54 (m, 2H), 8.24 (m, 2H), 8.35 (d, 2H, Ar, $J=2.4\text{ Hz}$), 8.90 (t, 2H, NH).

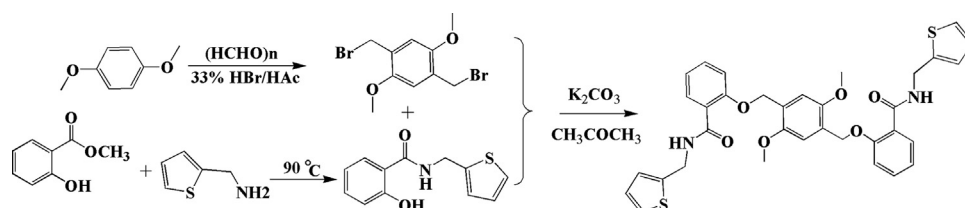
2.3. Synthesis of the complexes

$\{[\text{Gd}_2\text{L}_3(\text{NO}_3)_6] \cdot 2\text{C}_4\text{H}_8\text{O}_2\}_\infty$ (1). 62.8 mg (0.1 mmol) L and 39.9 mg (0.1 mmol) $\text{Gd}(\text{NO}_3)_3 \cdot 6\text{H}_2\text{O}$ were dissolved in a hot ethyl acetate solution to make a concentrated solution. Then the flask was cooled, and the mixture was filtered into a sealed 10–20 mL glass vial for crystallization at room temperature. After about two weeks, colorless single crystals of 1 suitable for crystal analysis were obtained. (yield: 72.0 mg, 56% based on $\text{Gd}(\text{NO}_3)_3 \cdot 6\text{H}_2\text{O}$). Analytical data (%), Calcd: C, 48.06; H, 4.11; N, 6.11; S, 7.00; Found: C, 48.18; H, 4.12; N, 6.13; S, 7.01; IR (KBr, ν , cm^{-1}): 3428(m), 2924 (m), 2852 (w), 1612 (s), 1564 (m), 1478 (s), 1300 (s), 1235 (m), 1030 (m), 988(m), 815 (w), 756 (m).

$\{[\text{Tb}_2\text{L}_3(\text{NO}_3)_6] \cdot 2\text{C}_4\text{H}_8\text{O}_2\}_\infty$ (2). The procedure was the same as that for Gd(III) complex using $\text{Tb}(\text{NO}_3)_3 \cdot 6\text{H}_2\text{O}$. Colorless single crystals were formed after three weeks. (yield: 57.8 mg, 45% based on $\text{Nd}(\text{NO}_3)_3 \cdot 6\text{H}_2\text{O}$). Analytical data (%), Calcd: C, 48.00; H, 4.10; N, 6.11, S, 6.99; Found: C, 48.09; H, 4.10; N, 6.12, S, 7.02. IR (KBr, ν): 3436 (m), 2925 (m), 1611 (s), 1561 (m), 1480(s), 1299 (s), 1223 (m), 1032 (m), 988 (m), 815 (w), 755 (m).

2.4. X-ray single-crystal diffraction analysis

Structure diffraction intensities of Gd(III) and Tb(III) complex were carried out on a Bruker SMART Apex CCD area detector diffractometer (Mo $\text{K}\alpha$, $\lambda=0.71073\text{ \AA}$) at 296 K. Data processing was accomplished with the SAINT processing program. Multiscan absorption corrections were applied by using the program SADABS [18]. The structures were solved with direct methods and refined with full-matrix least squares on F^2 using the SHELXL-97 program package [19]. All non-hydrogen atoms were subjected to anisotropic refinement, and all hydrogen atoms were added in idealized positions and refined isotropically. The R_1 values are defined as $R_1 = \frac{\sum \|F_o - |F_c|\|}{\sum F_o}$ and $wR_2 = \left\{ \frac{\sum [w(F_o^2 - F_c^2)^2]}{\sum [w(F_o^2)^2]} \right\}^{1/2}$. During the final steps of refinement high residual electron density was found near the thiophene, so the atoms of thiophene groups were considered to be disordered into two different positions. The disorder of terminal thiophene ring were treated by introducing a rigid bond restriction that forces both atoms to possess the same ADP parameters and their occupancies to be complementary modulated. Crystal parameters, data collection, and details concerning the structure refinement are summarized in Table 1,



Scheme 1. The synthetic route of the ligand L.

Table 1
Crystal data and structure refinement parameters for Tb(III) and Gd(III) complexes.

Empirical formula	C ₁₁₀ H ₁₁₂ Gd ₂ N ₁₂ O ₄₀ S ₆	C ₁₁₀ H ₁₁₂ N ₁₂ O ₄₀ S ₆ Tb ₂
Crystal system, space group	Triclinic, <i>P</i> -1	Triclinic, <i>P</i> -1
Unit cell dimensions	$a=12.5463(3)$ Å, $\alpha=98.475(5)^\circ$ $b=21.801(5)$ Å, $\beta=92.173(5)^\circ$ $c=23.015(5)$ Å, $\gamma=103.235(5)^\circ$	$a=12.5297(16)$ Å, $\alpha=98.434(2)^\circ$ $b=21.790(3)$ Å, $\beta=92.105(2)^\circ$ $c=22.969(3)$ Å, $\gamma=103.192(3)^\circ$
$V/\text{Å}^3$	6044(2)	6023.5(13)
$Z, D_{\text{calcd}}/\text{kg m}^{-3}$	2, 1.511	2, 1.518
μ/mm^{-1}	1.279	1.357
$F(0\ 0\ 0)$	2800	2804
Theta range for data collection/deg	1.79 to 25.02	1.73 to 25.02
Completeness to theta=25.05	98.1%	98.2%
Limiting indices	$-14 \leq h \leq 14, -25 \leq k \leq 25, -27 \leq l \leq 23$	$-13 \leq h \leq 14, -25 \leq k \leq 25, -27 \leq l \leq 25$
Reflections collected/unique	33510/20925 [$R(\text{int})=0.0379$]	33422/20887 [$R(\text{int})=0.0474$]
Data/restraints/params	20925/14/1655	20887/14/1655
Goodness-of-fit on F^2	1.055	1.018
Final R indices [$I > 2\sigma(I)$]	$R1=0.0594, wR2=0.1513$	$R1=0.0739, wR2=0.1976$
R indices (all data)	$R1=0.0896, wR2=0.1771$	$R1=0.1089, wR2=0.2342$
Largest diff. peak and hole($e/\text{Å}^3$)	2.306 and -1.603	1.934 and -1.239

representative bond lengths (Å) and angles ($^\circ$) are presented in Table S1. CCDC reference numbers 940194 and 940195. Graphics were drawn with DIAMOND (Version 3.2) [20].

3. Results and discussion

3.1. Synthesis

The semirigid ligand L was prepared by the ether base coupling of 1,4-bis(bromomethyl)-benzene and the thenylsalicylamide in a 1:2.25 ratio in dry acetone in the presence of an excess of anhydrous K_2CO_3 . One of the important issues in determining the framework structures is the geometry of the organic ligands. In our study, the terminal coordinating donors are separated by the benzene backbone at the para position, and two salicylamide arms are rotationally free and are thus capable of adjusting to match the metal coordination preference well. The new ligand gave satisfactory ^1H NMR, IR spectra, and elemental analyses. The syntheses of the complexes are straightforward. They were obtained by slow evaporation of ethyl acetate solution containing ligand L and corresponding lanthanide(III) ions. Within two weeks or longer time well-shaped colorless crystals suitable for X-ray analysis are separated in high yields. The complexes are soluble in DMF, DMSO, methanol and ethanol, slightly soluble in ethyl acetate, acetonitrile and acetone, but insoluble in CHCl_3 and ether. The characteristic band of the carbonyl group of free ligand L in IR spectra is shown at 1648 cm^{-1} . The absence of the band round 1648 cm^{-1} , which is instead of a new band at ca. 1611 cm^{-1} of the complexes compared to free ligands, indicates the complete coordination of the ligand. Weak absorptions observed in the range of $2900\text{--}2950\text{ cm}^{-1}$ can be attributed to the $\nu(\text{CH}_2)$ of the ligand. The absorption bands assigned to the coordinated nitrates were observed as two group bands at about 1480 cm^{-1} (ν_1) and 1300 cm^{-1} (ν_4) for the complexes. The differences between the strongest absorption band ν_1 and ν_4 of nitrate group lie in ca 180 cm^{-1} , indicating that coordinated nitrate groups in the complexes are bidentate ligands [21], the ν_3 of free nitrate group disappears in the spectra of the complexes, implying that three nitrate groups are all in coordination sphere which are further confirmed by X-ray crystallography as follows.

The room temperature PXRD patterns of the Gd(III) and Tb(III) complex of the ligand L as well as that of simulation for Tb(III) complex single crystal are unfolded from 5° to 50° as shown in Fig. 1. The powder XRD patterns of as-synthesized Gd(III) and Tb

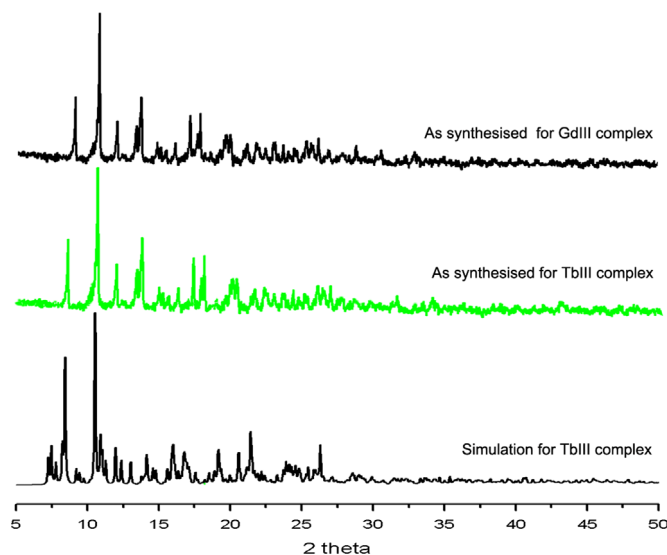


Fig. 1. Powder X-ray diffraction patterns of complexes.

(III) complex are almost identical to a pattern simulation from the single crystal data, which indicates the crystal structures are representative of the bulk material.

3.2. Crystal structure descriptions

Block crystals of Gd(III) and Tb(III) complex were obtained by reaction of $\text{Ln}(\text{NO}_3)_3 \cdot 6\text{H}_2\text{O}$ and L in ethyl acetate solution. X-ray crystal structure analyses reveal that Gd(III) and Tb(III) complex are isostructural and crystallize in the centrosymmetric triclinic space group *P*-1. Thus, only Tb(III) is selected for investigation here in detail as the representative example. The asymmetric unit of Tb(III) complex is composed of two crystallographically distinct Tb(III) metal centers, three ligands, six coordinating nitrate anions, and two ethyl-acetate solvent molecules. A first Tb(III) ion is nonacoordinated with three oxygen atoms from the carbonyl groups of three different ligands (Tb–O distances are 2.303(6), 2.313(6) and 2.331(6) Å), and three bidentately coordinating nitrate anion (Tb–O distances ranging from 2.428(7) to 2.547(8) Å) (Fig. 2a). The second Tb(III) ion is nonacoordinated as well, with three oxygen atoms from the carbonyl groups of another three different ligands (Tb–O distances are 2.301(6), 2.314(6) and 2.327(6) Å), and three bidentately coordinating nitrate anion (Tb–O

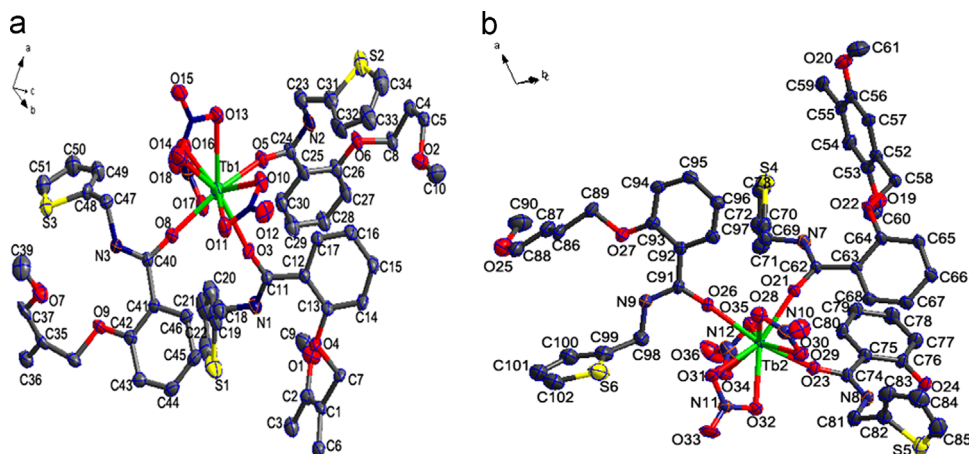


Fig. 2. The coordination environment of Tb1 (a) and Tb2 (b) with thermal ellipsoids at 30% probability (hydrogen atoms are omitted for clarity). Symmetry transformations: $i=x, y, z$; $ii=-x, -y, -z$. Color scheme: Tb atoms, green; C atoms, gray; O atoms, red; N atoms, blue; S atoms, yellow. (For interpretation of the references to color in this figure legend, the reader is referred to the web version of this article.)

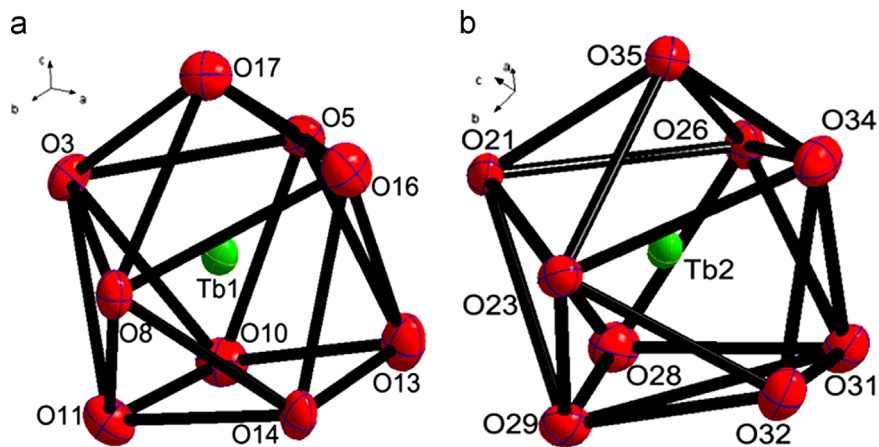


Fig. 3. The coordination polyhedron of Tb1 (a) and Tb2 (b).

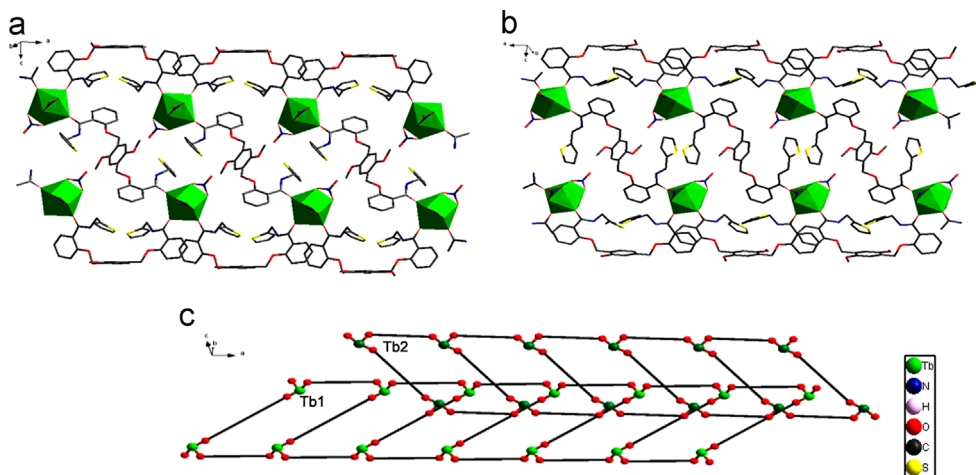


Fig. 4. Polyhedron presentation of 1D trapezoid ladder-like chain linked by ligands of Tb1 (a) and Tb2 (b). (Hydrogen atoms are omitted for clarity.) (c) Schematic representation of the 1D trapezoid ladder-like chains of Tb(III) complex (Gray nodes represent the anchors of the ligands).

distances ranging from 2.410(7) to 2.539(8) Å (Fig. 2b). For both Tb(III) ions, the coordination environment can be considered as a distorted square antiprism (Fig. 3). All of the bond lengths of Tb–O fall into the normal ranges. Unexpectedly, in the Tb(III) complex of L the ligand coordinate in a bidentate bridging mode with two ligands in a cis conformation and one ligand in a trans conformation which is unprecedented. The Tb...Tb distances bridged by ligand L with

deformed cis and trans conformation are ca. 12.529(7) and 18.752(7) Å, respectively, indicating that the trans conformation of L is more extended than the cis conformation. This arrangement of three ligands around the terbium ions leads to two trapezoid ladder-like chains with an intersection angle of 68.86° as shown in Fig. 4. The “T-shape” unit at Tb(III) center is slightly deviated from an ideal value ($O3-Tb1-O5=80.86(0)^\circ$, $O5-Tb1-O8=154.01(2)^\circ$, $O3-Tb1-O8=86.77$

(2)°, the Tb1–Tb1–Tb1 angles are 39.03(6)°, 140.96(4)°, 180.00(0)° and O21–Tb2–O23 = 83.23(5)°, O21–Tb2–O26 = 84.37(4)°, O23–Tb2–O26 = 154.66(0)°, the Tb2–Tb2–Tb2 angles are 42.59(3)°, 137.407(3)°, 180.00(0)°, respectively). It is worth to note that quadruple intermolecular hydrogen bonding interactions exist between the adjacent chains of the Tb1 and Tb2 as shown in Fig. 5. The oxygen atoms of two nitrate groups (O11, O14, O31 and O33) acted as hydrogen bond acceptor to interact with the hydrogen atom of the CH₃, thiophene and phenyl group (H9B, H9C, H22 and H78) to form an interesting three-dimensional supramolecular structures (Fig. 6). The distance between C7, C12, C24 and O1, O10, O6 is 3.529(8) Å, 3.460(3) Å, 3.416(4) Å and the corresponding C–H...O angle is 153.34(2)°, 151.09(6)° and 166.90(4)°. It is important to note that the etheric oxygen atoms of the two ligands are not coordinated to the Ln(III) center, but act as the hydrogen bonding acceptors to form strong intramolecular N–H...O hydrogen bonds which are stabilized by a stable 6-membered ring. The binding of lanthanide ions to the carbonyl oxygen atoms of ligands rather than to etheric oxygen groups appears largely as a consequence of the cooperative effect of strong intramolecular hydrogen bonds and steric hindrance inhibiting the formation of a reasonable coordination

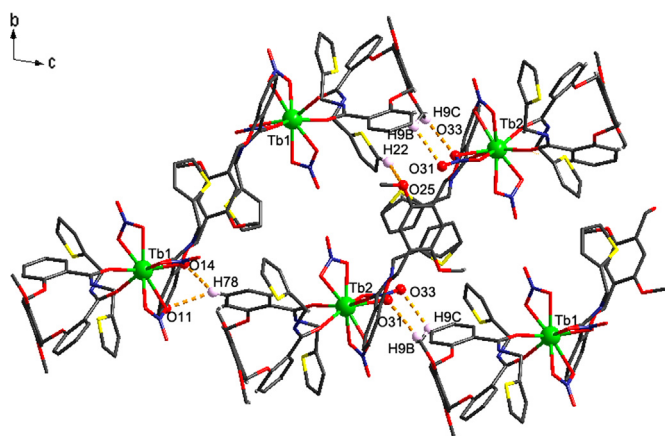


Fig. 5. C–H...O hydrogen bonding between Tb1 and Tb2 trapezoid ladder-like chains which are indicated with dashed yellow lines. (For interpretation of the references to color in this figure legend, the reader is referred to the web version of this article.)

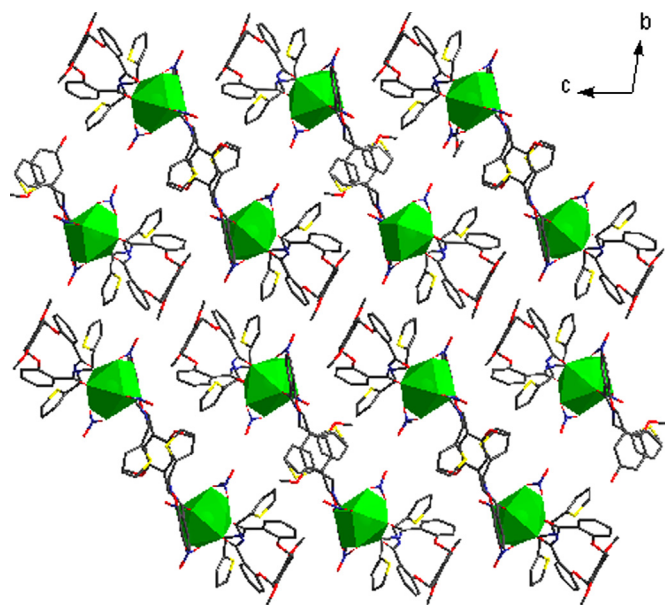


Fig. 6. The 3D supramolecular structure of Tb(III) complex constructed by C–H...O hydrogen bonds viewed from the crystallographic direction.

geometry that involves the participation of all two ether oxygen donors of each ligand which is characteristic of lanthanide compound of salicylamide ligands [11,12].

Compared with the structure of complex of similar ligand terminated with pyridine group [11k], terminal group-dependent structural variations are observed which can be understood taking into account the plastic coordinative behavior of this kind of ligands. By introduction of less electronegative thiophene group at the salicylamide arms in solvent system with weak coordination ability, the coordination behavior of the ligand was dramatically changed because of the presence of sulfur atoms which could make it less favorable for incorporating hydrogen bonds and affecting the coordination mode of the resulting bridging ligand. Consequently, each L ligand allowing the coordination of Ln(III) simultaneously by the two salicylamide arms of the ligands and thus the assembly of trapezoid ladder-like chains.

3.3. Luminescence properties

Taking into account the excellent luminescent properties of Tb(III) ions, the luminescence properties of Tb(III) coordination polymers and ligand L were investigated. As shown in Fig. 7, the free ligand L shows an emission band at 452 nm ($\lambda_{ex}=320$ nm) which is attributed to the $\pi \rightarrow \pi^*$ transitions. However, upon complexation with Tb(III) ions this emission is replaced by the typical luminescent color arising from Tb(III) cation. The excitation spectrum recorded from 250 to 530 nm (Fig. S1) shows a broad excitation band from 280 to 380 nm, originating from the organic ligand, as well as several weak sharp signals which can be assigned to direct Tb(III) excitation. While excitation was done at 325 nm, within the excitation band of the organic ligand, the emission spectrum only shows Tb(III) emission and no detectable emission of the organic ligand, thus confirming an efficient antenna effect for the luminescence of Tb(III) complex. A depiction of the green luminescence of the Tb(III) compound can be found in Fig. 8, the emission spectra of the Tb(III) compound shows the typical $f \rightarrow f$ based $^5D_4 \rightarrow ^7F_J$ transitions ($J=6-1$) at 478 and 482, 540 and 543, 576 and 582, 620 and 623, 644 and 648, and 672 nm as sharp signals, with the $^5D_4 \rightarrow ^7F_5$ emission at 543 nm as the emission maximum. The $^5D_4 \rightarrow ^7F_J$ transitions with $J=2-1$ around 648 and 672 are present but very weak in intensity.

In addition to steady-state measurements, the luminescence lifetimes of the Tb (3D_4) excited states and quantum yield determinations were determined. The lifetime of luminescence for Tb(III) complex was measured from the decay profile by fitting with

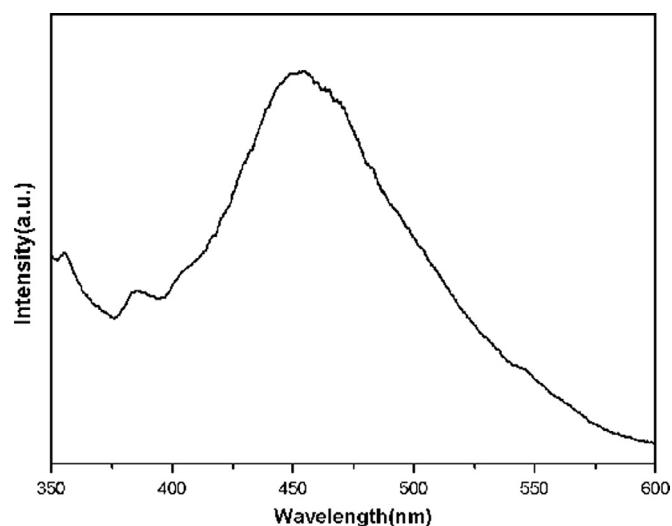


Fig. 7. Room-temperature emission spectra of ligand L ($\lambda_{ex}=320$ nm, excitation and emission passes = 0.2 nm) in the solid state.

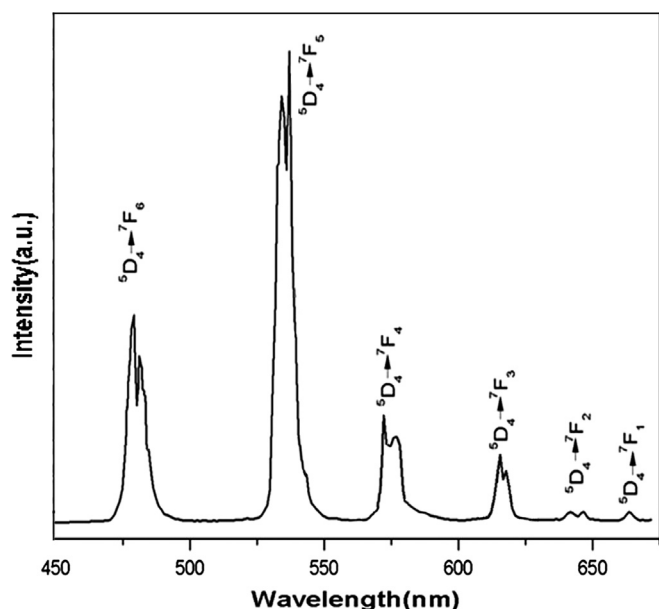


Fig. 8. Room-temperature emission spectra for terbium complex of ligand L ($\lambda_{\text{ex}}=325$ nm, excitation and emission passes=0.2 nm) in the solid state.

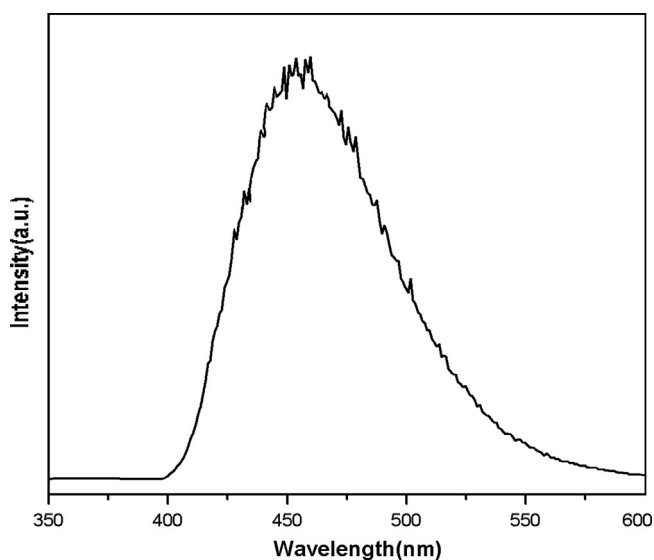


Fig. 9. Phosphorescence spectra of Gd(III) complex of ligand L in methanol-ethyl acetate solution at 77 K.

monoexponential decay curve with $\tau=1.34$ ms. The quantum yields of luminescence is 73%. The relatively longer luminescence lifetimes and larger quantum yield values are an indication that the bridging ligand provides a significant level of protection from nonradiative deactivation of lanthanide cations by the solvent molecules, as further supported by the energy transfer discussed below.

To demonstrate the energy transfer process, the phosphorescence spectrum of Gd(III) complex of L was measured for the triplet energy-level data. From the phosphorescence spectra (Fig. 9), the triplet energy level (${}^3\pi\pi^*$) of Gd(III) complex, which corresponds to its lower wavelength emission edge, is 24691 cm^{-1} (405 nm). Because the lowest excited state, ${}^6P_{7/2}$ ($E({}^6P_{7/2})=32000\text{ cm}^{-1}$) of Gd(III) is too high to accept energy from the ligand, the data obtained from the phosphorescence spectra actually reveal the triplet energy level of ligand in lanthanide complexes. In general, the sensitization pathway in luminescent terbium complexes consists of excitation of the ligands into their excited singlet states, subsequent intersystem

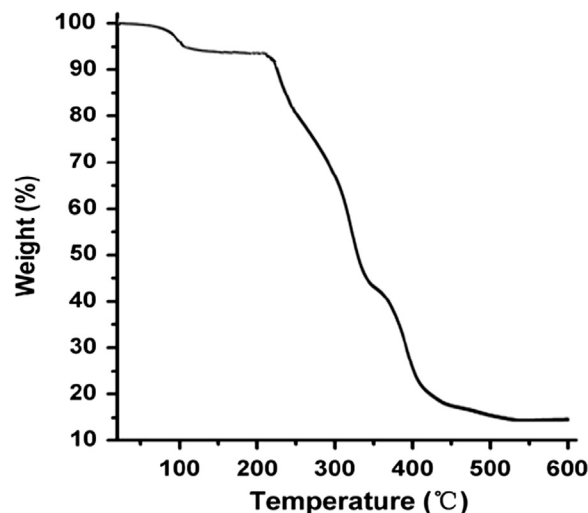


Fig. 10. TGA curves of Tb(III) complex.

crossing to their triplet states and energy transfer from the triplet state to the 5D_J manifold of the Tb(III) ions, followed by internal conversion to the emitting 5D_4 state. Finally, the Tb(III) ion emits when the $4f$ electrons undergo a transition from the excited state of 5D_4 to the 7F_J ground states ($J=6-1$). Latva's empirical rule [22] states that an optimal ligand-to-metal energy transfer process for Tb(III) needs $\Delta E={}^3\pi\pi^*-{}^5D_J$ ($2500-4500\text{ cm}^{-1}$). The triplet energy level of the ligand (24691 cm^{-1}) is higher than the 5D_4 level of Tb(III) (20400 cm^{-1}) and the energy gap ΔE is relatively large (about 4291 cm^{-1}), which points to an effective intersystem crossing process. This therefore supports the observation of stronger sensitization of the terbium complexes because of the larger overlap between the ligand triplet and terbium ion excited states.

Compared with the Tb(III) complex with the similar ligand terminated with picolysalicylamide group [11k], the luminescence lifetimes and quantum yields of Tb(III) complex are relatively longer and larger suggesting that one or more nonradiative pathways are assisting in the deactivation of the excited state and shortening the observed lifetimes, since the triplet energy level of the antenna only changed slightly, which excludes the possibility that the quenching of luminescence is due to a change in the nature of the antenna triplet state. The most probable explanation may be the former contain methanol molecules in the inner coordination sphere, which may quench Tb(III) emitting states.

3.4. Thermal properties

TGA have been carried out for two complexes which show similar behavior. The data of Tb(III) complex is taken as an example to be described in detail. As shown in Fig. 10, the thermal decomposition of Tb(III) complex occurs in a multi-step process from ambient temperature to $600\text{ }^\circ\text{C}$ to yield Tb_4O_7 as the final residue which is confirmed by the similar characteristic absorption of the residue in IR spectra compared with the standard sample spectrum of Tb_4O_7 (total weight loss: 86.26%; calculated: 86.41%). The first stage takes place from 25 to $118\text{ }^\circ\text{C}$, with a mass loss of 6.32% (calc. 6.39%), which corresponds to the loss of two ethylacetate molecules. Between 216 and $542\text{ }^\circ\text{C}$ a total weight loss of 79.94% corresponds to the thermal decomposition of the organic components and nitrate anions (calculated 80.01%). For Gd(III) complex the total weight loss was 86.49% with a calculated value of 86.76% between 25 and $523\text{ }^\circ\text{C}$.

4. Conclusions

We presented here a new semirigid bridging ligand featuring *N*-thenylamide arms which can form stable coordination polymers with lanthanide nitrates. The coordination polymers $\{[\text{Ln}_2(\text{NO}_3)_6\text{L}_3] \cdot 2\text{C}_4\text{H}_8\text{O}_2\}_\infty$ displays one dimensional trapezoid ladder-like chains built up from the connection of isolated $\text{LnO}_3(\text{NO}_3)_3$ polyhedra (distorted monocapped antisquare prism) through the ligand which can be further connected to interesting 3D supramolecular architecture by C–H...O hydrogen bonds. The luminescent properties of the Tb(III) complexes were investigated in detail. It is worthy noting that the bridging ligand provides a significant level of protection from nonradiative deactivation of lanthanide cations by the solvent molecules and exhibits a good antennae effect with respect to the Tb(III) ion due to efficient intersystem crossing and ligand-to-metal energy transfer. It seems that the terminal group as well as solvent system are all parameters of significant importance in coordination polymer synthesis. Our present findings provide the possibility of controlling the formation of the desired lanthanide coordination structure to enrich the crystal engineering strategy and enlarge the arsenal for developing excellent luminescent lanthanide complexes of salicylamide derivatives.

Supplementary material

Crystallographic data for the structural analysis have been deposited with the Cambridge Crystallographic Data Center, CCDC nos. 940194 and 940195. Copies of this information may be obtained free of charge from the director, CCDC, 12 Union Road, Cambridge CB2 1EZ, UK (e-mail: deposit@ccdc.cam.ac.uk or www: <http://www.ccdc.cam.ac.uk>).

Acknowledgments

This work was supported by the National Natural Science Foundation of China (Grants 21161011) and Gansu Natural Science Foundation of China (Grants 1212RJZA038).

Appendix A. Supporting information

Supplementary data associated with this article can be found in the online version at <http://dx.doi.org/10.1016/j.jssc.2013.07.014>.

References

- [1] O. Guillou, C. Daguebonne, Handbook on the Physics and Chemistry of Rare Earths, vol. 34, Elsevier, Amsterdam, 2005.
- [2] (a) J.Y. Lee, O.K. Farha, J. Roberts, K.A. Scheidt, S.T. Nguyen, J.T. Hupp, Chem. Soc. Rev. 38 (2009) 1450–1459; (b) C.L. Cahill, D.T. de Lill, M. Frish, Cryst. Eng. Comm 9 (2007) 15–26; (c) M.H.V. Werts, Sci. Prog. 88 (2005) 101–131; (d) H.C. Aspinall, Chem. Rev. 102 (2002) 1807–1850; (e) J.-G.G. Bünzli, S. Comby, A.-S. Chauvin, C.D.B. Vandevyver, J. Rare Earths 25 (2007) 257–274; (f) J. Yu, D. Parker, R. Pal, R.A. Poole, M.J. Cann, J. Am. Chem. Soc. 128 (2006) 2294–2299.
- [3] (a) J. An, C.M. Shade, D.A. Chengelis-Czegán, S. Petoud, N.L. Rosi, J. Am. Chem. Soc. 133 (2011) 1220–1223; (b) C. Marchal, Y. Filinchuk, X.Y. Chen, D. Imbert, M. Mazzanti, Chem. Eur. J. 15 (2009) 5273–5288; (c) X.J. Kong, Y.L. Wu, L.S. Long, L.S. Zheng, Z.P. Zheng, J. Am. Chem. Soc. 131 (2009) 6918–6919; (d) T. Devic, C. Serre, N. Audebrand, J. Marrot, G. Férey, J. Am. Chem. Soc. 127 (2005) 12788–12789; (e) L.J. Charbonnière, R. Ziessel, M. Guardigli, A. Roda, N. Sabbatini, M. Cesario, J. Am. Chem. Soc. 123 (2001) 2436–2437.
- [4] (a) X.J. Kong, L.S. Long, Z.P. Zheng, R.B. Huang, L.S. Zheng, Acc. Chem. Res. 43 (2010) 201–209; (b) M.D. Allendorf, C.A. Bauer, R.K. Bhakta, R.J.T. Houk, Chem. Soc. Rev. 38 (2009) 1330–1352; (c) C.M.G. dos Santos, A.J. Harte, S.J. Quinn, T. Gunnlaugsson, Coord. Chem. Rev. 252 (2008) 2512–2527; (d) T. Gunnlaugsson, J.P. Leonard, Chem. Commun. (2005) 3114–3113.
- [5] (a) M. Giraud, E.S. Andreiadis, A.S. Fisyuk, R. Demadrille, J. Pécaut, D. Imbert, M. Mazzanti, Inorg. Chem. 47 (2008) 3952–3954; (b) E.S. Andreiadis, R. Demadrille, D. Imbert, J. Pécaut, M. Mazzanti, Chem. Eur. J. 15 (2009) 9458–9476.
- [6] F.-Y. Yi, Q.-P. Lin, T.-H. Zhou, J.-G. Mao, Cryst. Growth Des. 10 (2010) 1788–1797.
- [7] (a) G.F. de Sá, O.L. Malta, C. de Mello Donegá, A.M. Simas, R.L. Longo, P.A. Santa-Cruz, E.F. da Silva Jr, Coord. Chem. Rev. 196 (2000) 165–195; (b) P.N. Remya, S. Biju, M.L.P. Reddy, A.H. Cowley, M. Findlater, Inorg. Chem. 47 (2008) 7396–7404; (c) D.B.A. Raj, B. Francis, M.L.P. Reddy, R.R. Butorac, V.M. Lynch, A.H. Cowley, Inorg. Chem. 49 (2010) 9055–9063; (d) S. Biju, D.B.A. Raj, M.L.P. Reddy, C.K. Jayasankar, A.H. Cowley, M. Findlater, J. Mater. Chem. 19 (2009) 1425–1432.
- [8] (a) M. Seitz, M.D. Pluth, K.N. Raymond, Inorg. Chem. 46 (2007) 351–353; (b) E.G. Moore, C.J. Jocher, J. Xu, E.J. Werner, K.N. Raymond, Inorg. Chem. 46 (2007) 5468–5470; (c) E.G. Moore, J. Xu, C.J. Jocher, I. Castro-Rodriguez, K.N. Raymond, Inorg. Chem. 47 (2008) 3105–3118; (d) A.P.S. Samuel, E.G. Moore, M. Melchior, J. Xu, K.N. Raymond, Inorg. Chem. 47 (2008) 7535–7544; (e) A.P.S. Samuel, J. Xu, K.N. Raymond, Inorg. Chem. 48 (2009) 687–698.
- [9] A.J. Amoroso, M.W. Burrows, R. Haigh, M. Hatcher, M. Jones, U. Kynast, K.M.A. Malik, D. Sendor, Dalton Trans. 16 (2007) 1630–1638.
- [10] (a) N. Chatterton, Y. Bretonnière, J. Pécaut, M. Mazzanti, Angew. Chem., Int. Ed. 44 (2005) 7595–7598; (b) G.S. Kottas, M. Mehlstäubl, R. Fröhlich, L.De Cola, Eur. J. Inorg. Chem. 22 (2007) 3465–3468; (c) L.J. Charbonnière, S. Mameri, D. Flot, F. Waltz, C. Zandanel, R.F. Ziessel, Dalton Trans. 22 (2007) 2245–2253; (d) L.S. Natrajan, P.L. Timmins, M. Lunn, S.L. Heath, Inorg. Chem. 46 (2007) 10877–10886; (e) L. Benisvy, P. Gamez, W.T. Fu, H. Kooijman, A.L. Spek, A. Meijerink, J. Reedijk, Dalton Trans. 24 (2008) 3147–3149; (f) N.M. Shavaleev, F. Gumy, R. Scopelliti, J.-C.G. Bünzli, Inorg. Chem. 48 (2009) 5611–5613; (g) R. Feng, F.-L. Jiang, M.-Y. Wu, L. Chen, C.-F. Yan, M.-C. Hong, Cryst. Growth Des. 10 (2010) 2306–2313.
- [11] (a) J. Zhang, Y. Tang, N. Tang, M.-Y. Tan, W.-S. Liu, K.-B. Yu, J. Chem. Soc., Dalton Trans. 14 (2002) 832–833; (b) Y. Tang, J. Zhang, W.-S. Liu, M.-Y. Tan, K.-B. Yu, Polyhedron 24 (2005) 1160–1166; (c) X.-Q. Song, W.-S. Liu, W. Dou, Y.-W. Wang, J.-R. Zheng, Z.-P. Zang, Eur. J. Inorg. Chem. 11 (2008) 1901–1912; (d) X.-Q. Song, W. Dou, W.-S. Liu, Y.-L. Guo, X.-L. Tang, Inorg. Chem. Comm. 10 (2007) 1058–1061; (e) Y.-W. Wang, Y.-L. Zhang, W. Dou, A.-J. Zhang, W.-W. Qin, W.-S. Liu, Dalton Trans. 39 (2010) 9013–9021; (f) Q. Wang, X. Yan, H. Zhang, W. Liu, Y. Tang, M. Tan, J. Solid State Chem. 184 (2011) 164–170; (g) X.-Q. Song, W.K. Dong, Y.J. Zhang, W.-S. Liu, Luminescence. 25 (2010) 328–335; (h) X.-Q. Song, L. Wang, Q.-F. Zheng, W.-S. Liu, Inorg. Chim. Acta 391 (2012) 171–178; (i) X.-Q. Song, L. Wang, M.-M. Zhao, G.-Q. Cheng, X.-R. Wang, Y.-Q. Peng, Inorg. Chim. Acta 402 (2013) 156–164; (k) X.-Q. Song, D.-Y. Xing, Y.-K. Lei, M.-M. Zhao, G.-Q. Cheng, X.-R. Wang, Y.-Q. Peng, Inorg. Chim. Acta. 404 (2013) 113–122.
- [12] (a) X.-Q. Song, W.-S. Liu, W. Dou, J.-R. Zheng, X.-L. Tang, H.-R. Zhang, D.-Q. Wang, Dalton Trans. 24 (2008) 3582–3591; (b) X.-Q. Song, X.-Y. Zhou, W.-S. Liu, W. Dou, J.-X. Ma, X.-L. Tang, J.-R. Zheng, Inorg. Chem. 47 (2008) 11501–11513; (c) X.-Y. Zhou, Y.-L. Guo, Z.H. Shi, X.-Q. Song, X.-L. Tang, X. Hu, Z.-T. Zhu, P.-X. Li, W.-S. Liu, W. Dou, Dalton Trans. 41 (2012) 1765–1775.
- [13] K. Nakagawa, K. Amita, H. Mizuno, Y. Inoue, T. Hakushi, Bull. Chem. Soc. Jpn. 60 (1987) 2037–2040.
- [14] F. Gutierrez, C. Tedeschi, L. Maron, J.-P. Daudey, R. Poteau, J. Azema, P. Tisnès, C. Picard, Dalton Trans. 9 (2004) 1334–1347.
- [15] M.S. Wrighton, D.S. Ginley, D.L. Morse, J. Phys. Chem. 78 (1974) 2229–2233.
- [16] K. Michio, Bull. Chem. Soc. Jpn. 49 (1976) 2679–2982.
- [17] Z. Jiri, P. Magdalena, H. Petr, T. Milos, Synthesis 110 (1994) 1132.
- [18] G.M. Sheldrick, SHELXS-97, Program for X-ray Crystal Structure Determination, University of Göttingen, Göttingen, Germany, 1997.
- [19] G.M. Sheldrick, SHELXL-97, Program for Crystal Structure Solution and Refinement, University of Göttingen, Göttingen, Germany, 1997.
- [20] K. Brandenburg, Diamond (Version 3.2), Crystal and Molecular Structure Visualization, (Ed.), K. Brandenburg and H. Putz Gbr, Crystal Impact, Bonn, Germany, 2009, <http://www.crystalimpact.com/diamond>.
- [21] K. Nakamoto, Infrared and Raman Spectra of Inorganic and Coordination Compounds, Wiley, New York, 2007.
- [22] M. Latva, H. Takalo, V.M. Mukkala, C. Matachescu, J.C. Rodriguez-Ubis, J. Kanakare, J. Lumin. 75 (1997) 149–176.